Rapid Formation of Superhydrophobic Surfaces with Fast Response Wettability Transition

Xiaotao Zhu,[†,‡] Zhaozhu Zhang,*,[†] Xuehu Men,[†] Jin Yang,[†,‡] and Xianghui Xu[†,‡]

State Key Laboratory of Solid Lubrication, Lanzhou Institute of Chemical Physics, Chinese Academy of Sciences, Tianshui Road 18th, Lanzhou 730000, P.R. China, and Graduate School, Chinese Academy of Sciences, Beijing 100039, P.R. China

ABSTRACT We have developed a facile and time-saving method to prepare superhydrophobic surfaces on copper sheets. Various surface textures composed of $Cu(OH)_2$ nanorod arrays and CuO microflowers/$Cu(OH)_2$ nanorod arrays hierarchical structure were prepared by a simple solution-immersion process. After chemical modification with stearic acid, the wettability of the as-prepared surfaces was changed from superhydrophilicity to superhydrophobicity. The shortest processing time for fabricating a superhydrophobic surface was 1.5 min. Interestingly, the rapid wettability transition between superhydrophobicity and superhydrophilicity can be realized on the prepared surfaces with ease by the alternation of air-plasma treatment and stearic acid coating. It took just 2 min to complete the whole wettability transition. Additionally, the regeneration of the superhydrophobic surface is also considered regarding its application.

KEYWORDS: superhydrophobic surface • rapid formation • air-plasma treatment • wettability transition • smart • regenerative

INTRODUCTION

Superhydrophobic surfaces with contact angles (CAs) more than 150° have attracted significant interest due to a wide range of potential applications (1−8). In nature, lotus leaves exhibit an unusual superhydrophobicity and self-cleaning property, called "lotus effect", resulting from the cooperative effect of the hydrophobic waxy coating and a binary surface roughness (9). To mimic this effect, researchers commonly fabricate artificial superhydrophobic surfaces in one of two general ways: either by creating hierarchical micro/nanostructures on the hydrophobic substrates (10, 11) or by chemically modifying a micro/nanostructured surface with low surface energy materials (12−14). On the basis of this principle, various methods have been reported for constructing the superhydrophobic surfaces such as anodic oxidation (15), plasma etching (16), electrospinning (17), sol−gel processing (18), and laser irradiation (19). However, these techniques all required either special equipment or complex process control. Jiang et al. (20) reported a simple method of fabricating a superhydrophobic surface on the copper substrate with the n-tetradecanoic. This process took a long time to carry out (about 3−5days), which limited the application of the superhydrophobic property on engineer material surfaces. In our present work, we simply and rapidly produced superhydrophobic surfaces on copper sheets, and the fast switchable wettability transition can be realized easily.

Smart surfaces with reversible switchable wettability under external stimuli are of great importance due to their numerous industrial applications (21−23). Upon environmental variations, such as electrical potential (24), solvents treatment (25), temperature treatment (26), light illumination (27, 28), and pH control (29), surface chemical and/or morphology of stimuli-sensitive materials can be changed, which results in the change of surface wetting behavior. However, the reversible wettability transitions triggered by above-mentioned approaches require a long time, even several weeks (28), which makes the switching less useful. Therefore, it would be desirable to realize the wettability transition rapidly. The work described below has accomplished this goal, and our new strategy has achieved the fast wetting reversible transition by the alternation of plasma treatment and chemical modification.

In this study, superhydrophobic surfaces were prepared by a simple solution-immersion process followed by chemical modification with the stearic acid. The shortest processing time for fabricating a superhydrophobic surface was 1.5 min. Reversible transition between superhydrophobic and superhydrophilic can be realized by the alternation of air-plasma treatment and stearic acid coating. The whole wettability transition is realized in a short time of 2 min. We expect that this simple and time-saving fabrication technique will make it possible for large-scale production of superhydrophobic engineering materials, and the rapid switchable wettability transition will find applications in smart devices.
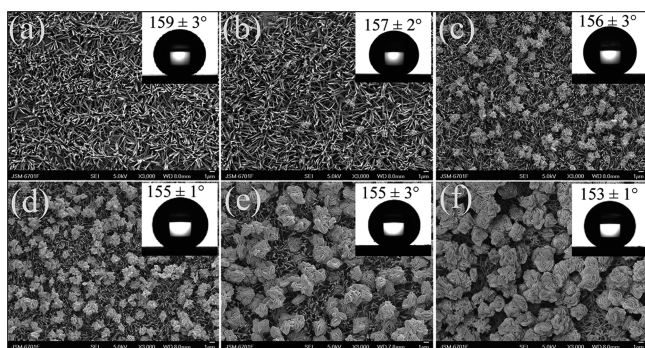
FIGURE 1. FESEM images of the sample surface after immersion in the solutions of NaOH and $(NH_4)_2S_2O_8$ for (a) 0.5, (b) 1, (c) 3, (d) 5, (e) 10, and (f) 20 min; the scale bars represent 1 μm in length. The insets correspond to water contact angles on each position.

EXPERIMENTAL SECTION

Materials. Copper sheet, sodium hydroxide (NaOH), ammonium persulphate $((NH_4)_2S_2O_8)$, stearic acid, acetone, and ethanol were of analytical grade and used as received.

Formation of Superhydrophobic Surfaces. Inspired by the previous method (30), $Cu(OH)_2$ nanorod arrays and CuO microflowers/$Cu(OH)_2$ nanorod arrays were prepared on the copper substrate. Briefly, the copper sheets were ultrasonically cleaned with acetone and deionized water sequentially and immersed into an aqueous solution of 2.5 M NaOH and 0.13 M $(NH_4)_2S_2O_8$ at room temperature for 0.5–20 min. During the immersion process, the color of the copper sheet surface turned gradually to faint blue, light blue, faint black, and light black. The copper sheets were then taken out from the solution and rinsed with deionized water, followed by drying under nitrogen. The as-prepared sample surfaces were immersed into a 0.006 M ethanol solution of stearic acid for 1 min. Subsequently, the copper sheets were rinsed by ethanol and blown to dry by nitrogen at room temperature.

Reversible Conversion of the Surface Wettability. The superhydrophobic surface was bombarded with air-plasma (1 W, low vacuum pressure of 5 Pa) for 1 min on a PGT-II plasmaapparatus. As a result, the wettability of the surface was converted into superhydrophilic. Then the plasma-treated surface was immersed in the ethanol solution of stearic acid for 1 min to restore the superhydrophobicity. The wettability transition between superhydrophobic and superhydrophilic was realized by the alternation of air-plasma treatment and stearic acid coating.

Characterization. Field-emission scanning electron microscopy (JEOL JSM-6701F FESEM) was used to observe the morphology of the $Cu(OH)_2$ nanorod arrays and CuO microflowers/$Cu(OH)_2$ nanorod arrays hierarchical structure. X-ray power diffraction (XRD) patterns were obtained using an X-ray diffractometer (Philips Corp., The Netherlands; operating with Cu Kα radiation at a continuous scanning mode and ω angle of 1.0°.). X-ray photoelectron spectroscopy (XPS) date was acquired using the VGESCALAB210 X-ray photoelectron spectrometer. The Mg Ka line ($h\nu = 1253.6$ eV) was used as the excitation source, and the binding energy 284.6 eV of C1s in hydrocarbon was used as reference. CAs and sliding angles (SAs) were measured by the sessile drop method using a KRÜSS DSA 100 (KRÜSS) apparatus. Water droplets (about 5–10 μL) were dropped carefully onto the surface. The average CA value was determined by measuring the same sample at five different positions. The image of the droplet was obtained by a digital camera (Canon).

RESULTS AND DISCUSSION

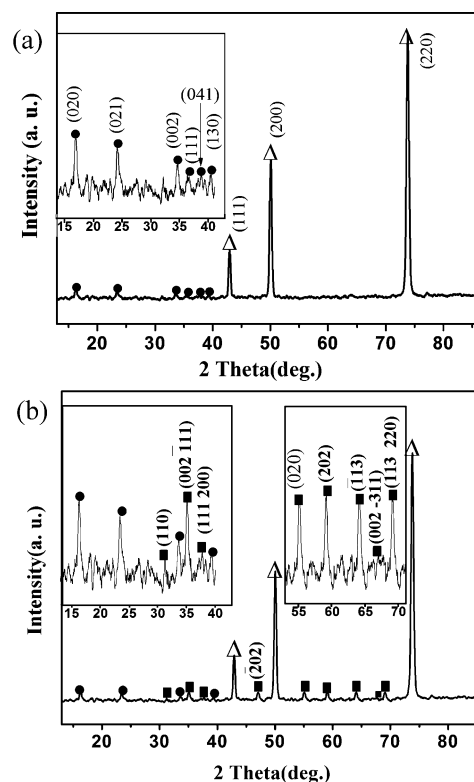Figure 1 shows the FESEM images of the sample surfaces after immersion in the NaOH and $(NH_4)_2S_2O_8$ aqueous

FIGURE 2. XRD pattern of (a) $Cu(OH)_2$ nanorod arrays and (b) CuO/$Cu(OH)_2$ hierarchical structure on the copper substrate. The insets correspond to the magnified diffraction peaks in the region 10–40° and 50–70°.

solution for (a) 0.5, (b) 1, (c) 3, (d) 5, (e) 10, and (f) 20 min. Obviously, the immersion time plays a crucial role in determining the surface structure. After 0.5 min of immersion, the surface of the copper sheet is uniformly covered with nanorod arrays (Figure 1a). When the immersion time is prolonged to 1 min and above, the hierarchical structures of microflowers and nanorod arrays on the copper substrate are formed. It is seen that the microflowers are standing on the nanorod arrays, and the size and density of the microflowers are increasing with extending reaction time (Figure 1b–f). XRD analysis is carried out to study the crystal structure of nanorod arrays and microflowers/nanorod arrays hierarchical structure on the copper substrate (Figure 2). As seen in Figure 2a (the crystal structure of the nanorod arrays; the corresponding FESEM image is shown in Figure 1a), all the peaks marked with black dots, positioned at 2θ values of 10–40°, are indexed to orthorhombic $Cu(OH)_2$ (JCPDS card No. 72–0140), except those marked with triangles arising from the copper substrate. Figure 2b presents the XRD pattern of the microflowers/nanorod arrays hierarchical structure (the corresponding FESEM images are shown in Figure 1b–f). Comparing the XRD pattern of $Cu(OH)_2$ nanorod arrays, eight new peaks marked with rectangles in the region 33–70° appear. The new diffraction peaks are indexed as the (110), (002 $\bar{1}$11), (111 200), (020), (202), ($\bar{1}$13), (002 $\bar{3}$11), and (113 220) plane of the monoclinic-phase CuO (JCPDS card No. 80–0076). From the XRD analysis, it can be concluded that the nanorod arrays and the microflowers/nanorod arrays hierarchical structure are

ACS APPLIED MATERIALS & INTERFACES

3637

composed of $Cu(OH)_2$ crystals and $Cu(OH)_2/CuO$ crystals, respectively.

In alkaline aqueous solution, the surfaces of the copper sheets are rapidly oxidized to Cu^{2+} by the oxidant $(NH_4)_2S_2O_8$, and the reaction that accounts for the $Cu(OH)_2$ nanorod arrays formation is essentially an oxidation process (30).

$$Cu + 4NaOH + (NH4)_2S_2O_8 \rightarrow Cu(OH)_2 + 2Na_2SO_4 + 2NH_3 \uparrow + 2H_2O$$
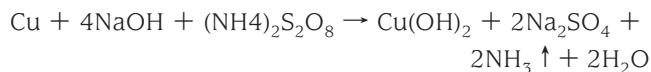
The formation of the $Cu(OH)_2$ nanorod arrays depends mainly on the concentration of NaOH and $(NH_4)_2S_2O_8$ (31), and the growth rate of the controllable morphologies can be controlled by the reaction time (30−33). We took the solution of 2.5 M NaOH and 0.13 M $(NH_4)_2S_2O_8$ as a model system. In the initial stage, nanoparticles and some nanorods were formed, and then some bamboo-shoot-like rods emerged (32). In the following stage, nanorod arrays were formed, and the length of the rods increased with the time (30−33). During the next stage, some microflowers were synchronously deposited from the bulk solution because of the reaction of Cu^{2+} ions resulting from copper oxidation and OH^- during the growth of the nanorods. Simultaneously, some of the microflowers were transfixed by several nanorods (32), and the size and density of the microflowers increased with the time as mentioned above.

The as-prepared sample surfaces were superhydrophilic with the CAs of almost 0°. After immersion in the stearic acid solution for 1 min, these surfaces exhibited superhydrophobicity, with the static CAs ranging from 159° to 153° (insets in Figure 1). The CAs almost remained unchanged even the water volume changing from 5 to 10 μL. Moreover, the CAs were still more than 150° after three months storage at ambient conditions, indicating the good long-term stability of the surfaces. Water droplets were easy to slide off with the SAs less than 5° on the as-prepared superhydrophobic surfaces. Moreover, when a droplet of 10 μL hit the surfaces, it can bounce away from the surfaces. Along the continuous bounce on the surfaces, the water droplet moved from left to right rapidly (Figure 3), indicating the surface possessing robust superhydrophobicity under dynamic wetting. It is well-known that improving the surface roughness is a crucial factor in the fabrication of superhydrophobic surfaces (34). The nanorod arrays or hierarchical structures on the copper sheet can trap a large fraction of air within the grooves, which is important for the formation of superhydrophobicity. As a contrast, we observed that the CA of the smooth copper surface only reached to 109° after modification with stearic acid. It should be noted that this fabrication method makes it possible to fabricate a superhydrophobic surface on copper substrates within 2 min, which would be very advantageous for the industrial large-scale production.

Interestingly, the surface wettability of the samples with different immersion time was found to exhibit rapid reversible transition by the alternation of air-plasma treatment and stearic acid coating, allowing it to be changed between
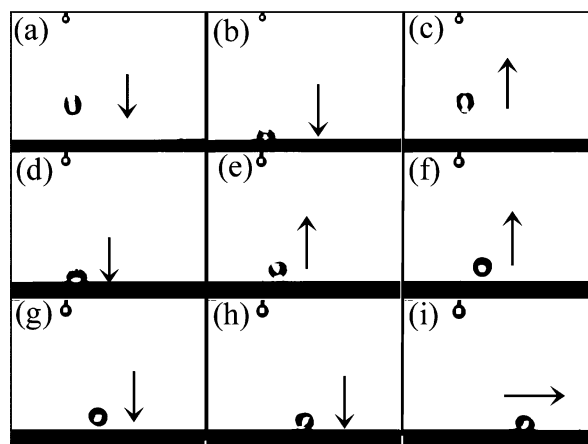

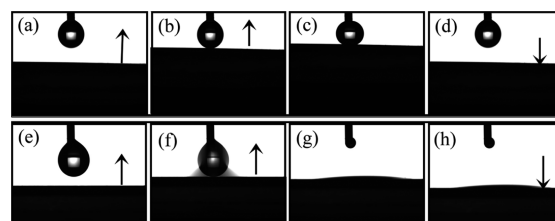FIGURE 3. Snapshots of a 10 μL water droplet vertically hitting the superhydrophobic $CuO/Cu(OH)_2$ surface.

FIGURE 4. Approach, contact, deformation, and departure process of a 5 μL water droplet suspending on a syringe with respect to the surfaces: (a−d) the as-prepared superhydrophobic surfaces; (e−h) the air-plasma-treated surfaces. The arrows represent the moving direction of the substrate.

superhydrophobicity and superhydrophilicity quickly. We take the sample surface obtained by immersion in the NaOH and $(NH_4)_2S_2O_8$ aqueous solution for 0.5 min as a model system. Before plasma treatment, a water droplet (5 μL) suspending on a syringe was difficult to be pulled down to the surface in all cases, even though the droplet was deformed severely (Figure 4a−d). Upon air-plasma treatment, the superhydrophobic surface was converted into a superhydrophilic one. When a water droplet was dropped onto the surface, it spread out on the surface immediately, with the time of 0.3 s (Figure 4e−h). However, when the plasma-treated surface was immersed in the stearic acid solution, the superhydrophobicity of surface was obtained again, with the CA restoring to 159°. It just took 2 min to fulfill the whole switchable wettability transition. Rapid wettability transition is a very important characteristic to enable the application of surface in terms of smart devices, such as controlled transportation of fluids, water-proof coatings for moisture-sensitive electronic devices, rapid water motion, and smart membranes. This process had been repeated several times, and the good reversibility of the surface wettability was observed (Figure 5).

To thoroughly understand the source of wettability change, the changes of the surface compositions and the microstructure of the surface were investigated. The morphology of the surface was the same before and after experiencing air-plasma treatment. This means that the wettability variation may result from the changes of surface compositions. The starting surface was fully covered with a stearic acid monolayer, making the surface superhydrophobic. The sharp
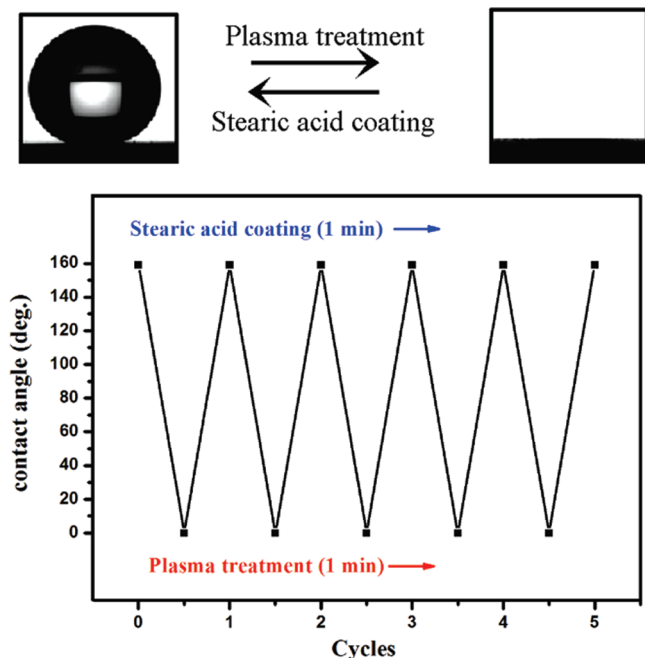
FIGURE 5. Reversible wettability transition can be rapidly realized through plasma treatment and stearic acid coating, respectively.

wettability change after air-plasma plasma treatment was caused by a local chemical change, which was verified by the XPS analysis. Spectra a and c in Figure 6 show the survey XPS spectra of the surfaces before and after air-plasma treatment, respectively. It can be seen that the C 1s, O 1s, and Cu 2p peaks are detected for both the surfaces before and after air-plasma treatment and the amount of relative of oxygen increases after plasma treatment. To get more information on the changes of the surface compositions, we collected high-resolution XPS data for O 1s and C 1s. As it is shown in spectra b and d in Figure 6, the multielement spectra of O 1s is resolved into four components centered

at BE = 530.4, 531.7, 532.7, and 533.9 eV, which are ascribed to Cu−O, Cu−OH, C−O, and −COO species, respectively (35−37). It can be seen that the content of the C−O and −COO species increases after air-plasma treatment, with the value increasing from 28.2 to 32.7% and 9.3 to 32.3%, respectively. Figure 7 shows the multielement spectra of C1s, which are fitted to different peaks attributable to different chemical states, namely, C−C/C−H, C−O, and O−C=O. From the fitted results, it is seen that the original content of the C−O and O−C=O groups is low, with 14.3 and 12.4%, respectively (Figure 7a), whereas the value increases to 19.6 and 25.3% after air-plasma treatment for 1 min (Figure 7b). It is well-known that plasma containing electrons, ions, radicals, and neutral molecules strongly interacts with the surfaces, and as a result, chemical modification occurs on the surfaces (38). Among various plasma treatments, oxidative (oxygen and air) plasma treatment is found to be an effective tool for improving wettability by creating −COOH, −CO, and other relevant groups (39). As a result, the surface hydrophilic is improved, and the CA of the surface changes from 159 to 0°.

The most distinctive characteristic of the process is its reversibility by a simple stearic acid coating process, which is realized rapidly. Upon immersion in the stearic acid solution, the plasma-treated surface came back to the original superhydrophobic state. It is supposed that upon stearic acid coating, the surface is fully covered with the alkyl chains again. The XPS also demonstrates that after coating with stearic acid, the content of the −CH₃ group increased almost to the original value (Figure 7c).

With respect to the real application, the superhydrophobic surface is easily scratched, especially upon contamination with hard contact. Additionally, unlike the plant leaves, the destroyed surfaces almost cannot be repaired automatically, which limits the applications of the superhydrophobic
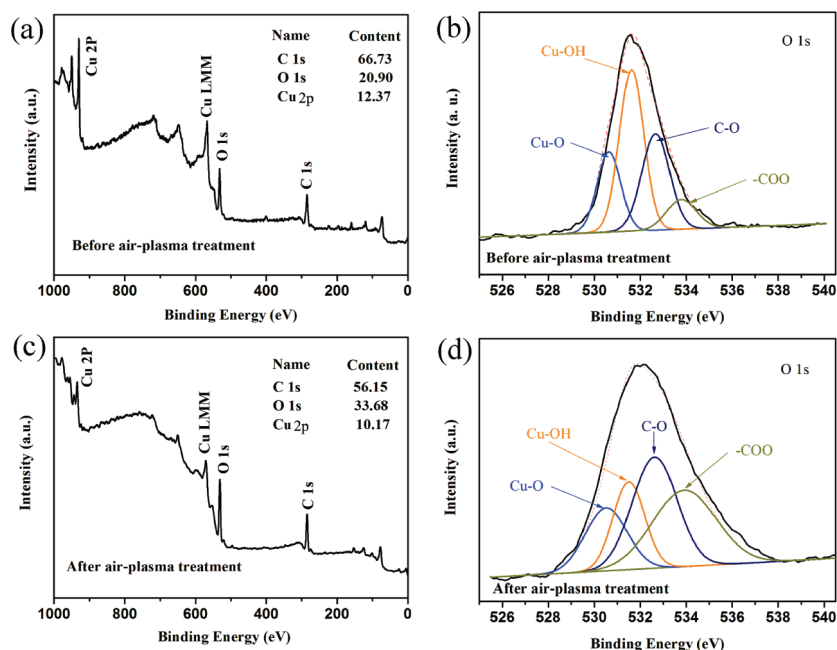

FIGURE 6. XPS survey spectrum and O 1s XPS spectrum of the surface (a, c) before and (b, d) after air-plasma treatment, respectively.

FIGURE 8. Photographs of water droplets (a) on the surface partly destroyed by mechanical scratching and (b) on the regenerated surface by immersion in NaOH and $(NH_4)_2S_2O_8$ aqueous solution and stearic acid coating again.

be emphasized that the reparative surface also shows fast wettability transition property by the alternation of air-plasma treatment and stearic acid coating.

CONCLUSION

In summary, superhydrophobic surfaces were fabricated on the copper substrate by a facile and time-saving approach. The shortest processing time for fabrication of a superhydrophobic surface was 1.5 min. By the alternation of air-plasma treatment and stearic acid coating, the rapid reversible wettability transition of the surface between superhydrophobicity and superhydrophilicity was realized. XPS analysis demonstrated that oxygen species were incorporated in the surface after air-plasma treatment. The whole wetting transition procedure was accomplished within 2 min. Meanwhile, the fabrication process is so facile and time-saving that it provides an opportunity to construct a regenerative superhydrophobic surface. We expect that this fabrication technique could perhaps show the most promise for the widest array of applications as it can be applied to the large-scale production, it do not typically require expensive materials and complicated application methods, and it can be easily used to repair the damaged superhydrophobic surfaces. Moreover, the rapid wetting transition may have significant application potential, especially in the smart microfluidic devices.
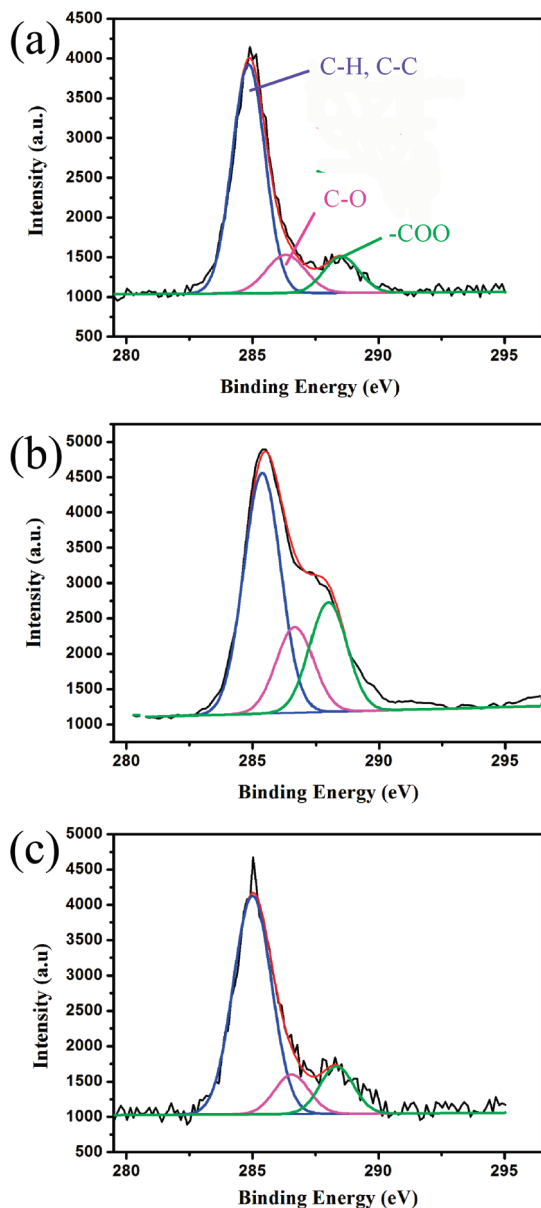
FIGURE 7. XPS of the C1s level (a) before plasma treatment, (b) after plasma treatment, and (c) after stearic acid coating, respectively.

surface. How to regenerate the superhydrophobic performance of a surface after being scratched becomes a key concern. The alternative way would be to prepare superhydrophobic surfaces with simple fabrication and easy repairability. In this work, the prepared superhydrophobic surfaces can also be damaged by the mechanical scratch. However, as the fabrication approach is facile and time-saving, it provides an opportunity to construct a regenerative superhydrophobic surface. As shown in Figure 8a, when the superhydrophobic surface was damaged in some area by a knife, the CA decreased sharply to about 100°. After being treated again by immersion in NaOH and $(NH_4)_2S_2O_8$ aqueous solution and the stearic acid coating process, the damaged surface was rendered with superhydrophobicity. The reparative surface can restore its good superhydrophobicity with the CA of 159° (Figure 8b). The easy repairability is expected to satisfy the future demands in the practical application of superhydrophobicity. Additionally, it should
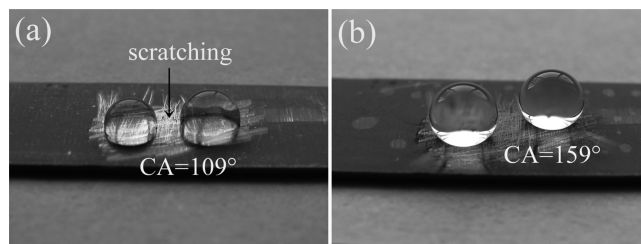
REFERENCES AND NOTES

(1) Li, X. M.; Reinhoudt, D.; Crego-Calama, M. *Chem. Soc. Rev.* **2007**, *36*, 1350–1368.
(2) Erbil, H. Y.; Avcl, Y.; Mert, O. *Science* **2003**, *299*, 1377–1380.
(3) Parker, A. R.; Lawrence, C. R. *Nature* **2001**, *414*, 33–34.
(4) Feng, X. J.; Feng, L.; Jin, M. H.; Zhai, J.; Jiang, L.; Zhu, D. B. *J. Am. Chem. Soc.* **2004**, *126*, 62–63.
(5) Pan, Q. M.; Wang, M. *ACS Appl. Mater. Interfaces* **2009**, *1*, 420–423.
(6) Hong, X.; Gao, X.; Jiang, L. *J. Am. Chem. Soc.* **2007**, *129*, 1478–1479.
(7) Shirtcliffe, N. J.; McHale, G.; Newton, M. I.; Zhang, Y. *ACS Appl. Mater. Interfaces* **2009**, *1*, 1316–1323.
(8) Gao, L.; McCarthy, T. J. *Langmuir* **2006**, *22*, 2966–2967.
(9) Barthlott, W.; Neinhuis, C. *Planta* **1997**, *202*, 1–8.
(10) Jin, M.; Feng, L.; Sun, T. L.; Zhai, J.; Li, T.; Jiang, L. *Adv. Mater.* **2005**, *14*, 1977–1981.

(11) Lee, J. A.; McCarthy, T. J. *Macromolecules* **2007**, *40*, 3965–3969.

(12) Huang, L.; Lau, S. P.; Yang, H. Y.; Leone, E. S. P.; Yu, S. F.; Prawer, S. J. *J. Phys. Chem. B.* **2005**, *109*, 7746–7748.

(13) Larmour, I. A.; Bell, S. E. J.; Saunders, G. C. *Angew. Chem., Int. Ed.* **2007**, *46*, 1710–1712.

(14) Bhushan, B.; Jung, Y. C.; Koch, K. *Langmuir* **2009**, *25*, 3240–3248.

(15) Thieme, M.; Frenzel, R.; Schmidt, S.; Simon, F.; Henning, A.; Worch, H.; Lunkwitz, K.; Scharnweber, D. *Adv. Eng. Mater.* **2001**, *3*, 691–695.

(16) Lejeune, M.; Lacroix, L. M.; Bretagnol, F.; Valsesia, A.; Colpo, P.; Rossi, F. *Langmuir* **2006**, *22*, 3057–3661.

(17) Singh, A.; Steely, L.; Allock, H. R. *Langmuir* **2005**, *21*, 11604–11607.

(18) Tadanaga, K.; Morinaga, J.; Matsuda, A.; Minami, T. *Chem. Mater.* **2000**, *12*, 590–592.

(19) Kietzig, A. M.; Hatzikiriakos, S. G.; Englezos, P. *Langmuir* **2009**, *25*, 4821–4827.

(20) Wang, S. T.; Feng, L.; Jiang, L. *Adv. Mater.* **2006**, *18*, 767–770.

(21) Daniel, S.; Chaudhury, M. K.; Chen, J. C. *Science* **2001**, *291*, 633–636.

(22) Beebe, D. J.; Moore, J. S.; Yu, Q.; Liu, R. H.; Kraft, M. L.; Jo, B.-H.; Devadoss, C. *Proc. Natl. Acad. Sci. U. S. A* **2000**, *97*, 13488–13493.

(23) Russell, T. P. *Science* **2002**, *297*, 964–967.

(24) Krupenkin, T. N.; Taylor, J. A.; Schneider, T. M.; Yang, S. *Langmuir* **2004**, *20*, 3824–3827.

(25) Lu, X. Y.; Peng, J.; Li, B. Y.; Zhang, C. C.; Han, Y. C. *Macromol. Rapid Commun.* **2006**, *27*, 136–141.

(26) Song, W. L.; Xia, F.; Bai, Y. B.; Liu, F. Q.; Sun, T. L.; Jiang, L. *Langmuir* **2007**, *23*, 327–331.

(27) Wang, S. T.; Feng, X. J.; Yao, J. N.; Jiang, L. *Angew. Chem., Int. Ed.* **2006**, *45*, 1264–1267.

(28) Caputo, G.; Cortese, B.; Nobile, C.; Salerno, M.; Cingolani, R.; Gigli, G.; Cozzoli, P. D.; Athanassiou, A. *Adv. Funct. Mater.* **2009**, *19*, 1149–1157.

(29) Wang, S. T.; Liu, H. J.; Liu, D. S.; Ma, X. Y.; Fang, X. H.; Jiang, L. *Angew. Chem., Int. Ed.* **2007**, *46*, 3915–3917.

(30) Zhang, W. X.; Wen, X. G.; Yang, S. H.; Berta, Y.; Wang, Z. L. *Adv. Mater.* **2003**, *15*, 822–826.

(31) Hou, H. W.; Xie, Y.; Li, Q. *Cryst. Growth. Des.* **2005**, *5*, 201–205.

(32) Chen, X. H.; Kong, L. H.; Dong, D.; Yang, G. B.; Yu, L. G.; Chen, J. M.; Zhang, P. Y. *J. Phys. Chem. C* **2009**, *113*, 5396–5401.

(33) Wen, X. G.; Zhang, W. X.; Yang, S. H. *Langmuir* **2003**, *19*, 5898–5903.

(34) Zhu, W. Q.; Feng, X. J.; Feng, L.; Jiang, L. *Chem. Commun.* **2006**, *26*, 2753–2755.

(35) Sarkar, D. K.; Paynter, R. W. *J. Adhes. Sci. Technol.* **2010**, *24*, 1181–1189.

(36) Xu, T.; Yang, S. R.; Lv, J. J.; Xue, Q. J.; Li, J. Q.; Guo, W. T.; Sun, Y. Y. *Diamond. Relat. Mater.* **2001**, *10*, 1441–1447.

(37) Balazs, D. J.; Triandafillu, K.; Wood, P.; Chevolot, Y.; van Delden, C.; Harms, H.; Hollenstein, C.; Mathieu, H. J. *Biomaterials* **2004**, *25*, 2139–2151.

(38) Chai, J. A.; Lu, F. Z.; Li, B. M.; Kwok, D. Y. *Langmuir* **2004**, *20*, 10919–10927.

(39) Tsougeni, K.; Papageorgiou, D.; Tserepi, A.; Gogolides, E. *Lab Chip* **2010**, *10*, 462–469.